Test of the Jarzynski and Crooks Fluctuation Relations in an Electronic System

O.-P. Saira,[1,2] Y. Yoon,[1] T. Tanttu,[2] M. Möttönen,[1,2] D. V. Averin,[3] and J. P. Pekola[1]

[1]*Low Temperature Laboratory (OVLL), Aalto University, P.O. Box 15100, FI-00076 Aalto, Finland*
[2]*Department of Applied Physics/COMP, Aalto University, P.O. Box 14100, FI-00076 Aalto, Finland*
[3]*Department of Physics and Astronomy, Stony Brook University, SUNY, Stony Brook, New York 11794-3800, USA*

Recent progress on micro- and nanometer-scale manipulation has opened the possibility to probe systems small enough that thermal fluctuations of energy and coordinate variables can be significant compared with their mean behavior. We present an experimental study of nonequilibrium thermodynamics in a classical two-state system, namely, a metallic single-electron box. We have measured with high statistical accuracy the distribution of dissipated energy as single electrons are transferred between the box electrodes. The obtained distributions obey Jarzynski and Crooks fluctuation relations. A comprehensive microscopic theory exists for the system, enabling the experimental distributions to be reproduced without fitting parameters.

Everyday concepts such as heat and mechanical work have their foundation in dynamics at the atomic and molecular scale, which is typically unobservable in macroscopic samples. Advances in the synthesis and manipulation of biological matter have made it possible to study the response of individual molecules [1] to mechanical forces; also see Ref. [2] for a recent review. In these experiments, the external force is modulated following a predetermined protocol and the resulting work W exerted upon the system is measured. Consequently, the fluctuating nature of the thermodynamic quantity ''work'' is revealed, as repeated measurements yield different results depending on the microscopic trajectory traversed by the molecule. Similar studies have been performed on colloidal particles [3] and mechanical oscillators [4]. Fluctuation theorems such as the Jarzynski equality (JE) [5] enable one to infer path-independent equilibrium free-energy differences from the statistics of irreversible measurement protocols. The JE states that

$$\langle e^{-W/k_B T} \rangle = e^{-\Delta F/k_B T}, \qquad (1)$$

where the ensemble average is taken over repetitions of the force protocol starting from an equilibrium state at temperature T, and ΔF is the difference in free energy between the final and initial values of the external control parameters. As we demonstrate experimentally, this equation applies also to a single-electron device operated in a dilution refrigerator at temperatures of about 200 mK. An electrostatic gate drive plays the role of the time-dependent mechanical force that has been missing in previous studies of fluctuation theorems in electronic systems [6] and is crucial for studying JE (1) and Crooks fluctuation relations discussed below.

The system that is the subject of our study is a single-electron box [7] as depicted in the scanning electron micrograph of Fig. 1(a). The box is formed by two metallic electrodes that are electrically connected through a tunnel junction with a small electric capacitance C_j. The complete circuit diagram and naming of capacitors is shown in Fig. 1(b). The sole degree of freedom that is of interest here is the number n of electrons transferred from the left to the right electrode. The relevant n-dependent part of the electrostatic energy of the single-electron box is given by [8]

$$U = E_c(n^2 - 2nn_g), \qquad (2)$$

where $E_c = e^2/(2C_\Sigma)$ is the characteristic unit of charging energy of the box, e is electron charge, $C_\Sigma = C_j + C_g$ is the total capacitance of the box, $C_g = (C_L^{-1} + C_R^{-1})^{-1}$ is the effective gate capacitance, and $n_g = C_g V_g/e$ is the gate charge in units of e. The charge number n changes by ± 1 in the process of electron tunneling across the junction. In the temperature range of strong Coulomb blockade $T \ll E_c/k_B$, thermal excitations of n are exponentially unlikely when the gate charge n_g in Eq. (2) is an integer [7]. Thus, the charge number n can be driven between two adjacent charge states, for example, $n = 0$ and $n = 1$, by a protocol $n_g(t)$ that ramps the gate charge between the values $n_g = 0$ and $n_g = 1$. This is demonstrated in Fig. 1(c).

We employ a readout that yields the heat $Q = W - \Delta U$ deposited into the electrodes in such driven transitions. The theoretical analysis presented in Refs. [8,9] establishes that JE can be written in terms of Q as

$$\langle e^{-Q/k_B T} \rangle = 1, \qquad (3)$$

provided that the drive protocol is such that the $n = 0 \rightarrow 1$ transition always occurs. This condition is realized in the present experiment to an accuracy of 10^{-4} (see Supplemental Material [10]). For completeness, we illustrate in Fig. 1(d) the relationship between Q and the dissipated work $W_{\text{dis}} = W - \Delta F$ appearing in the fluctuation
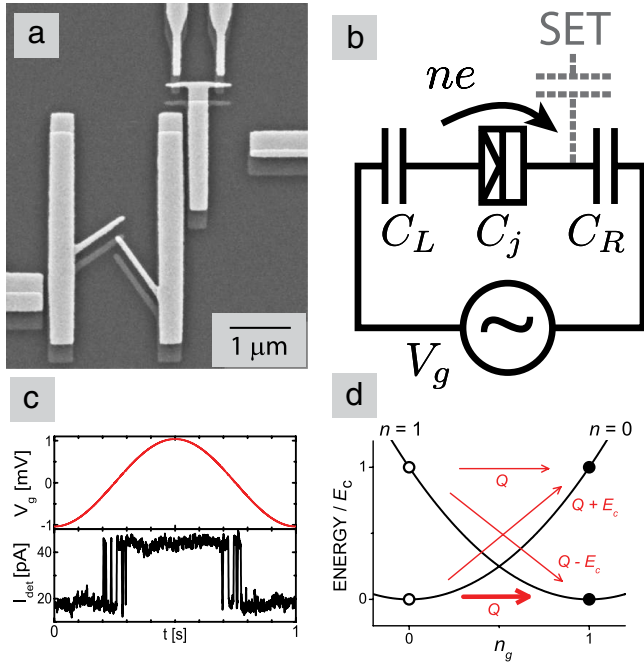
FIG. 1 (color online). (a) Scanning electron micrograph of the active area of the measured sample, which shows metallic films fabricated on an oxidized silicon wafer by e-beam lithography and shadow evaporation technique [18]. Two shifted copies of the original resist mask pattern lie on the surface: copper layer appears brighter compared to oxidized aluminum. Tunnel junctions are formed in the overlap regions between the two films. The single-electron box is located on the left, and the SET electrometer is at the top. The tips of two gate electrodes that are used to control the electrostatics of the box and the electrometer are visible at the left and right edges. (b) Simplified circuit diagram of the system. The galvanically isolated single-electron box is connected capacitively to its environment via C_L and C_R and to the electrometer as illustrated by the dashed gray line. (c) Full period of the sinusoidal drive signal (top) applied to the control gate, and one instance of electrometer response (bottom). The drive frequency is 1 Hz, and the amplitude is equal to one gate modulation period of the box. (d) Energy-level diagram of the system for the two lowest-energy charge states. Black parabolas represent the charging energy of the system in the states $n = 0$ and $n = 1$ as a function of the externally controlled gate charge n_g. The arrows indicate possible combinations of initial and final states (open and filled circles, respectively). The expression for dissipated work $W - \Delta F$ is given next to the arrow for each trajectory type, illustrating that work separates into dissipated heat Q and change of internal energy.

relations for other trajectory types as well. One can similarly write the Crooks fluctuation theorem [11] in terms of Q as

$$\frac{P_F(-Q)}{P_R(Q)} = e^{-Q/k_B T}, \qquad (4)$$

where P_F and P_R are the probability distributions of Q when the system is driven in forward (F) or reverse (R)

directions, respectively. Importantly, the above formulations of the fluctuation theorems can be applied without detailed knowledge of the internal dynamics of the system, thus retaining their universality and usefulness.

Charge tunneling is governed thermally by the excitations of conduction electrons in the box electrodes that couple to the bath of lattice phonons. Hence, switching dynamics between the different charge states n is dissipative. The amount of energy deposited into the two electrodes in a single tunneling event equals the difference of the chemical potentials of the electrodes at the time of the tunneling, which is essentially instantaneous on the other relevant time scales in the problem [12]. The chemical potential difference is given by the change in energy U of Eq. (2) in response to a change $\Delta n = \pm 1$ of the charge number n. In general, the n trajectory consists of a random number N of successive back-and-forth tunneling events, and hence the total heat generated in such a trajectory is [9]

$$Q = 2E_c \sum_{k=1}^{N} \pm \left[n_g(\tau_k) - \frac{1}{2} \right], \qquad (5)$$

where τ_k is the stochastic time instant of the kth tunneling event, and the sign is the same as for Δn in the event. Because of the intrinsic randomness of the tunneling events, the heat Q fluctuates from one gate voltage ramp to another. In the experiment, the system was driven with a sinusoidal excitation corresponding to $n_g(t) = \frac{1}{2} - \frac{1}{2} \cos(2\pi f t)$ with frequencies f ranging from 1 to 20 Hz. These frequencies are sufficiently slow that at the turning points of the drive, i.e., when $n_g(t) = 0$ or 1, the system occupies the minimum energy charge state $n = n_g(t)$ with high probability. Hence, each half cycle from 0 to 1 and similarly from 1 to 0 can be considered an independent realization of the control protocol.

We perform the heat readout by detecting the electron tunneling events by a capacitively coupled single-electron transistor (SET) (see Supplemental Material [10]). Equation (5) yields the heat Q in terms of E_c for an individual $n_g(t)$ sweep. One can thus utilize the experimental Q distributions in two ways: with the use of the values of E_c and T determined by independent means, the validity of Eqs. (3) and (4) can be tested. On the other hand, accepting Eqs. (3) or (4), one can determine the ratio $E_c/k_B T$ and furthermore find E_c by multiplying this ratio with the independently measured temperature of the sample holder.

The preceding discussion is independent of the details of the charge tunneling rates in the single-electron box. However, in our case it is possible to analyze the fluctuation relations also from a microscopic point of view. Charge transport through $Cu/AlO_x/Al$ normal-metal–insulator–superconductor (N-I-S) tunnel junctions occurs via thermally activated $1e$ events described by the orthodox theory [12], provided that (i) the tunneling resistance R_T of the junction is high compared to the resistance quantum

$R_K \simeq 25.8$ kΩ, (ii) quasiparticles in the electrodes obey an equilibrium thermal distribution, and (iii) coupling of stray microwaves to the junction has been prevented by appropriate shielding and filtering in the construction of the sample stage and signal lines. Realization of these conditions in N-I-S single-electron devices, including the backaction from the capacitively coupled electrometer, has been studied in detail in recent years [13,14]. Based on these studies, nonthermal charge transport is expected to be negligible at least above temperatures of 150 mK. In particular, overheating of the superconducting electrode in the present design is diminished by the fact that quasiparticle excitations can relax to the overlapping normal metal through the oxide barrier. Observed stochastic switching of the system between charge states at a fixed value of gate charge near degeneracy can be directly fitted to the tunneling rates predicted by the orthodox theory (see Supplemental Material [10]). We extract values $\Delta = 218 \pm 3$ μeV, $E_c/k_B = 1.94 \pm 0.05$ K, and $R_T = 100 \pm 13$ MΩ for the superconducting gap parameter, charging energy of the box, and tunneling resistance of the box junction, respectively. For the detector SET, we obtain $R_T = 0.63$ MΩ and $\Delta = 211$ μeV from a fit to the measured I-V characteristics.

The experimentally obtained Q distributions for drive frequencies 1, 2, and 4 Hz are presented in Fig. 2(a). The distributions were measured at a bath temperature of 214 mK where the thermally activated tunneling rate at degeneracy was 70 Hz, which is well within the detector bandwidth of about 1 kHz. In addition, we have similar data but in smaller quantities for driving frequencies from 5 Hz to 20 Hz. At frequencies higher than this, the observed distributions deviate significantly from the theoretical prediction due to systematic errors arising from finite readout bandwidth and uncertainty in the event timing. On the other hand, driving frequencies lower than 1 Hz make the measurement susceptible to $1/f$ type charge noise that is ubiquitous in metallic single-electron devices [15]. In Fig. 2(a), we show also the exact theoretical distributions based on charge kinetics described by the orthodox theory and sample parameters obtained in the manner described above. The theoretical and experimental distributions are in excellent agreement.

To assess quantitatively the systematic error due to finite detector bandwidth, we also show in Fig. 2(a) the distributions obtained from Monte Carlo simulations that incorporate a finite detector rise time before threshold detection. Visually, the change in the shape of the distribution functions appears small. Quantitatively, we can assess the accuracy of the readout by evaluating the exponential average $\langle e^{-Q/k_B T} \rangle$, which equals 1 for the ideal thermally activated kinetics. From the Monte Carlo simulations, we obtain 1.006 for the 1 and 2 Hz cases and 1.012 for the 4 Hz case. For the experimental distributions, evaluation of the Jarzynski average yields 1.033 ± 0.003 (for 1 Hz drive),
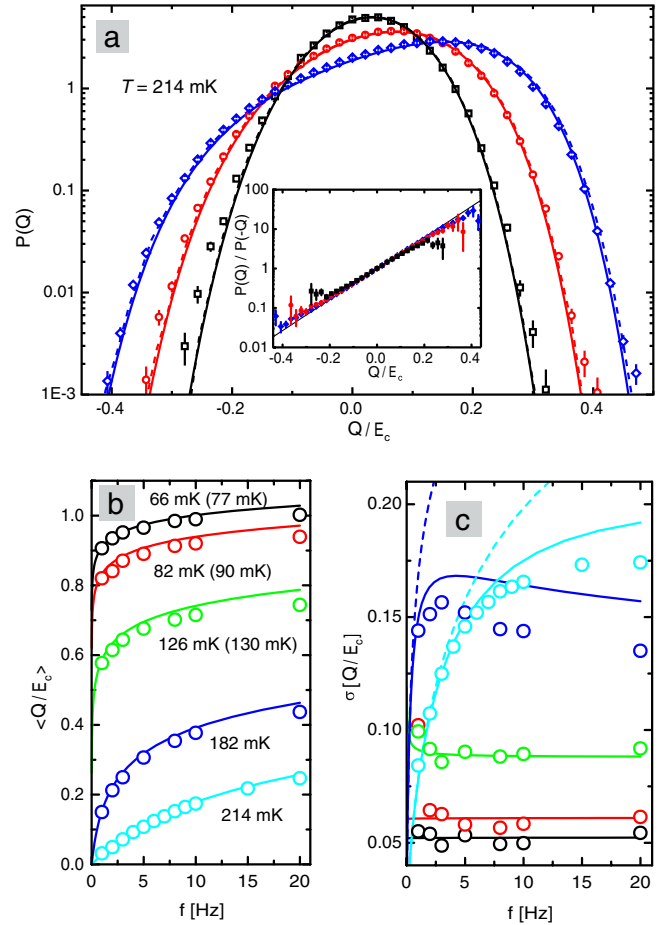

FIG. 2 (color online).   (a) Measured distribution of the generated heat at drive frequencies 1 Hz (black squares), 2 Hz (red circles), and 4 Hz (blue diamonds). The solid lines are exact theoretical predictions for the independently determined sample parameter values. The dashed lines show the results of Monte Carlo simulations, where the finite bandwidth of the detector was included in the model. Inset: $P(Q)/P(-Q)$ ratio for the experimental distributions. Solid line shows the result from the Crooks fluctuation theorem. [(b) and (c)] First and second moments, respectively, of the Q distribution at different drive frequencies and bath temperatures. Markers are experimental data, and solid lines are exact theoretical predictions as in part (a). For the lowest bath temperatures, the theoretical curves have been calculated using a slightly elevated electron temperature to account for nonideal thermalization as discussed in the text. The temperature used in the calculation is given in parentheses if it differs from the sample stage temperature. In panel (c), dashed lines represent the distribution width inferred from the FDT formula $\langle (Q - \langle Q \rangle)^2 \rangle = 2kT\langle Q \rangle$ using the theoretical value of the first moment $\langle Q \rangle$.

1.032 ± 0.003 (2 Hz), and 1.044 ± 0.004 (4 Hz), when using the independently determined $E_c/k_B T$ ratio as described above. The stated uncertainty is the unbiased estimate for the standard deviation of the mean based on the observations, not including the uncertainty of the value of $E_c/k_B T$. As the relative uncertainty of the independent E_c

estimate is 3%, the JE is shown to hold within experimental accuracy, accounting for the 1% bias from finite detector bandwidth. Conversely, starting from the assumption that JE holds for the experimental distributions, we obtain an estimate $E_c/k_B = 1.91 \pm 0.03$ K.

The possibility to numerically evaluate the theoretical Q distribution to a high accuracy enables us to assess the magnitude of sampling error in the experiment. From the acquired experimental data, the distribution can be determined reliably for a range of Q/E_c values where $P(Q) > 10^{-3}$. Evaluating numerically the contribution to JE outside this interval, we see that the deviation due to sampling errors is of the order 10^{-3}.

Concerning the Crooks fluctuation theorem in the form of Eq. (4), the forward and backward distributions coincide in the present case of a gate drive that is antisymmetric with respect to the degeneracy point. Hence, we present the experimental $P(Q)/P(-Q)$ ratio as a function of heat Q in the inset of Fig. 2(a). On a semilogarithmic plot, one expects a linear dependence with the slope equal to $1/k_BT$, independent of frequency. The experimental data adheres to this quite well, but there is a tendency towards less steep slopes for a lower frequency. This feature can be reproduced in our simulations by assuming a broadening of the Q distributions due to an additive Gaussian noise having a rms amplitude of $0.0035E_c = 0.032k_BT$ independent of driving frequency. We attribute the broadening to the residual background charge noise that induces fluctuations in the exact position of the degeneracy point.

In Figs. 2(b) and 2(c), we present the mean generated heat $\mu = \langle Q \rangle$ and distribution width $\sigma = \sqrt{\langle (Q - \mu)^2 \rangle}$ for different bath temperatures in the range of 66–214 mK and drive frequencies 1–20 Hz. The experimental results agree well with the values obtained from numerical simulations performed in the same manner as for Fig. 2(a). Theoretical results for the moments of Q distribution are presented in Ref. [9] for a normal state box, and similar results hold for the first two moments in the present N-I-S case as well. For sufficiently low f values, the box remains close to local equilibrium during the gate voltage drive. In this case, the transfer of heat Q into the box reservoirs can be viewed as a linear response to small deviations from the equilibrium caused by the drive. As a linear response, this process satisfies the classical fluctuation-dissipation theorem (FDT) which takes the form $\sigma = \sqrt{2k_BT\mu}$. This implies that in the adiabatic limit, the generated heat vanishes not only on average but for all individual tunneling trajectories. Local equilibrium also implies that the distribution of heat Q is Gaussian [9], similar to all equilibrium thermodynamic fluctuations. The behavior is evident in the experimental data for $T = 182$ and 214 mK, where the slowest drive frequencies produce an almost Gaussian Q distribution, whereas the distributions become strongly non-Gaussian as the frequency is increased. At lower temperatures, the adiabatic threshold frequency is well

below 1 Hz and thus inaccessible in the present experiment. For the simulations at the lowest temperatures, we had to use somewhat higher temperatures than those indicated by the sample stage thermometer in order to reproduce the experimental data [see Fig. 2(b)]. At low temperatures, charge kinetics is expected to depart from the basic thermal activation model with a single heat bath, as discussed earlier. Note that our test of the fluctuation relations is not carried out in this regime.

Thermodynamics of the driven transitions in electronic systems studied in this work will play an important role in the development of reversible information processing devices [16]. We also envision this work to introduce a fruitful test bed of nonequilibrium fluctuation theorems in qualitatively new settings such as engineered environments. It is possible to realize experimentally a regime where the charge transitions are dominated by coupling to an external nonequilibrium environment [13]. A fully superconducting box [17] should enable the study of thermodynamic fluctuations in true quantum regime, which at the moment is mostly an unexplored territory for experiments.

---

[1] J. Liphardt, S. Dumont, S. B. Smith, I. Tinoco, Jr., and C. Bustamante, Science **296**, 1832 (2002); D. Collin, F. Ritort, C. Jarzynski, S. B. Smith, I. Tinoco, and C. Bustamante, Nature (London) **437**, 231 (2005); I. Junier, A. Mossa, M. Manosas, and F. Ritort, Phys. Rev. Lett. **102**, 070602 (2009).

[2] A. Alemany, M. Ribezzi, and F. Ritort, AIP Conf. Proc. **1332**, 96 (2011).

[3] G. M. Wang, E. M. Sevick, E. Mittag, D. J. Searles, and D. J. Evans, Phys. Rev. Lett. **89**, 050601 (2002); V. Blickle, T. Speck, L. Helden, U. Seifert, and C. Bechinger, Phys. Rev. Lett. **96**, 070603 (2006).

[4] F. Douarche, S. Ciliberto, A. Petrosyan, and I. Rabbiosi, Europhys. Lett. **70**, 593 (2005).

[5] C. Jarzynski, Phys. Rev. Lett. **78**, 2690 (1997).

[6] N. Garnier and S. Ciliberto, Phys. Rev. E **71**, 060101(R) (2005); Y. Utsumi, D. S. Golubev, M. Marthaler, K. Saito, T. Fujisawa, and G. Schön, Phys. Rev. B **81**, 125331 (2010); B. Küng, C. Rössler, M. Beck, M. Marthaler, D. S. Golubev, Y. Utsumi, T. Ihn, and K. Ensslin, Phys. Rev. X **2**, 011001 (2012).

[7] D. V. Averin and K. K. Likharev, J. Low Temp. Phys. **62**, 345 (1986); M. Büttiker, Phys. Rev. B **36**, 3548 (1987); P. Lafarge, H. Pothier, E. R. Williams, D. Esteve, C. Urbina, and M. H. Devoret, Z. Phys. B **85**, 327 (1991).

[8] J. Pekola and O.-P. Saira, J. Low Temp. Phys. **169,** 70 (2012).

[9] D. V. Averin and J. P. Pekola, Europhys. Lett. **96,** 67004 (2011).

[10] See Supplemental Material at http://link.aps.org/supplemental/10.1103/PhysRevLett.109.180601 for a detailed description of data analysis and supporting theory.

[11] G. E. Crooks, Phys. Rev. E **60,** 2721 (1999).

[12] D. V. Averin and K. K. Likharev, in *Mesoscopic Phenomena in Solids*, edited by B. L. Altshuler, P. A. Lee, and R. A. Webb (Elsevier, Amsterdam, 1991), p. 173; G.-L. Ingold and Y. V. Nazarov, in *Single Charge Tunneling: Coulomb Blockade Phenomena in Nanostructures*, edited by H. Grabert and M. H. Devoret (Plenum Press, New York, 1992), p. 21.

[13] O.-P. Saira, M. Möttönen, V. F. Maisi, and J. P. Pekola, Phys. Rev. B **82,** 155443 (2010).

[14] O.-P. Saira, A. Kemppinen, V. F. Maisi, and J. P. Pekola, Phys. Rev. B **85,** 012504 (2012).

[15] B. Starmark, T. Henning, T. Claeson, P. Delsing, and A. N. Korotkov, J. Appl. Phys. **86,** 2132 (1999).

[16] S. Toyabe, T. Sagawa, M. Ueda, E. Muneyuki, and M. Sano, Nature Phys. **6,** 988 (2010); G. Schaller, C. Emary, G. Kiesslich, and T. Brandes, Phys. Rev. B **84,** 085418 (2011); D. V. Averin, M. Möttönen, and J. P. Pekola, Phys. Rev. B **84,** 245448 (2011).

[17] Y. Nakamura, Yu. A. Pashkin, and J. S. Tsai, Nature (London) **398,** 786 (1999).

[18] T. A. Fulton and G. J. Dolan, Phys. Rev. Lett. **59,** 109 (1987).